International Journal of Theoretical Physics (2023) 62:237
https://doi.org/10.1007/s10773-023-05498-3

RESEARCH

Quantum Heat Engine with Level Degeneracy for Oscillator-shaped Potential Well

Yaman Evkaya[1] · **Özgür Ökcü**[2,3] · **Ekrem Aydiner**[2,3]

Received: 11 September 2023 / Accepted: 16 October 2023 / Published online: 7 November 2023
© The Author(s), under exclusive licence to Springer Science+Business Media, LLC, part of Springer Nature 2023

Abstract
In this paper, we consider positive oscillator-shaped well potential and set a Szilard-like quantum heat engine based on energy level degeneracy. By using position-dependent energy eigenvalues of the oscillator-shaped well, we compute extracted work and efficiency based on Stirling-like thermodynamical cycle. We obtain numerical results for physical quantities and discuss work and efficiency dependence of angular frequency, well width, and temperature.

Keywords Quantum heat engine · Position dependent mass · Szilard engine

1 Introduction

The notion of Maxwell's demon has played a vital role in the understanding of thermodynamics, information and computing. Maxwell contemplated a Gedanken experiment where he discussed a possible violation of the second law of thermodynamics [1]. The first objection to Maxwell's gedanken experiment came from Szilárd in 1929 [2]. He investigated Maxwell's idea with an imaginary device known as the Szilárd engine which consists of a gas molecule inside an enclosed box. A thin and frictionless barrier is inserted in the middle of box. A demon controls the barrier and lets the particles move from one part to another part of the box. Szilárd showed that the second law of thermodynamics is valid. However, measurement of the particle position gives rise to entropy decrease in an amount of $k_B \ln 2$. In order to explain the increase of entropy, Launder proposed an erase principle which states that the erasure or reset of

✉ Ekrem Aydiner
ekrem.aydiner@istanbul.edu.tr

Yaman Evkaya
yevkaya@hotmail.com

Özgür Ökcü
ozgur.okcu@ogr.iu.edu.tr

[1] TEBİP High Performers Program, İstanbul University, 34134 İstanbul, Türkiye

[2] Department of Physics, Faculty of Science, Istanbul University - Istanbul, 34134 İstanbul, Türkiye

[3] Theoretical and Computational Physics Research Laboratory, İstanbul University, İstanbul, Türkiye

the demon's memory cost minimum energy in an amount of $k_B T \ln 2$ [3]. Hence, it prevents to decrease in the entropy for each measurement, and the total entropy of system increases[3–6]. Using a single colloidal particle, Landauer's principle was tested experimentally in Ref. [7]. In Ref. [8], it was experimentally shown that the required work to erase the memory is nearly $k_B T \ln 2$ for a single electron engine. Moreover, many experimental studies revealed the Szilard engine producing positive work [8–13].

On the other hand, experimental progressions in quantum physics bring thermodynamics to smaller scales [14, 15]. For example, quantum heat engines are the microscopic generalization of the classical heat engines which convert the heat into work according to the laws of quantum statistical mechanics. In contrast to classical heat engines, quantum heat engines are modeled as systems having discrete energy levels. The first quantum heat engine was proposed as a three-level maser [16]. Diverse classical heat engines such as Otto, Carnot, Stirling, Brayton and Diesel were generalized to quantum case [17–28]. Interestingly, quantum heat engines beyond the Carnot efficiency have been proposed without violating the second law of thermodynamics [29–36]. Quantum heat engine models were also proposed for various working medium such as multilevel quantum systems [37–39], particle in a box [40] and harmonic oscillator [41–44]. Kim et al. firstly proposed quantum Szilárd engine where a thin barrier is inserted and removed in the middle of the box [45]. Then, it has been shown that positive work and efficiency can be obtained in the studies devoted to quantum Szilárd engines [45–50].

Another interesting aspect of quantum heat engines is the level of degeneracy. Using level degeneracy, it is possible to obtain more work and efficiency than the nondegeneracy case. For instance, Mehta and Johal considered a quantum Otto heat engine with an interacting two-level system with degeneracy [51]. They found that the degeneracy case is more efficient than the nondegeneracy case. Based on the level degeneracy, the quantum Szilard engine was studied for infinite well potential by Thomas et al. [52]. They found the work and efficiency depend on the width of well. In the low-temperature limit, they showed that efficiency approaches the Carnot limit. Based on Ref. [52], quantum Szilard heat engines were studied for harmonic oscillator potential [53, 54], fractional power-law potential and fractional dynamics [55, 56], identical particles [57].

It is also interesting to extend the study of Ref. [52] under the different potentials. More recently, the authors have studied two exact solutions of non-rectangular quantum well, namely the oscillator-shaped well potential in Ref. [58]. It is well known that there are not any solutions of Schrödinger equations for the coupling case of harmonic oscillators and infinite well problems. However, an exact solution is possible under the assumption of position-dependent mass, i.e., if the mass of the quantum system varies with position [59–70]. Indeed, the position-dependent mass plays a very important role in many physical systems such as semiconductors [71], superlattices [72], materials of non-uniform chemical composition [73], heterostructures [74], and abrupt heterojunctions [75]. It would be interesting to examine the heat engines in oscillator-shaped quantum well systems since position dependent mass systems have a wide field of applications. Moreover, energy levels depend on both angular frequency and well boundaries [58]. Therefore, based on these motivations, we would like to handle the quantum Szilárd engine for oscillator-shaped quantum well potential.

The paper is organized as follows: In the next section, we briefly mention the quantum Szilárd engine based on level degeneracy. Then, we compute the work and efficiency for two energy levels of an oscillator-shaped well. Finally, we give our results and a brief discussion in the last section.

2 Stirling-like Cycle

A Stirling cycle includes four successive paces of isothermal and isochoric processes [52]. In Fig. 1, we present the dynamics of a Stirling cycle.

Stage 1: We begin to consider box A with a single particle in a heat bath at hot temperature T_h. During the isothermal process *AB*, a thin barrier is quasistatically inserted in the middle of the box, thus the system remains in equilibrium with a hot heat bath at the same temperature T_h.

Stage 2: Then, box B behaves like double-well potentials. In the isochoric process *BC*, the system connects the cold heat bath at temperature T_c.

Stage 3: Next, the thin barrier is quasistatically removed in the isothermal process *CD*, thus the system is in thermal equilibrium with a cold heat bath at temperature T_c, and box D behaves like single well potential again.

Stage 4: Finally, the system is connected to hot heat bath at temperature T_h. It undergoes heat absorption in the isochoric process *DA* and is completed.

The corresponding partition functions of boxes *A* and *D* are given by

$$Z_{A/D} = \sum_{n=0}^{\infty} e^{-\beta_{h/c} E_n}, \tag{1}$$

where $\beta_{h/c} = \frac{1}{k_B T_{h/c}}$, E_n is the energy level of the system, and *h*/*c* denotes the hot and cold, respectively. On the other hand, the partition functions of boxes *B* and *C* are given by

$$Z_{B/C} = \Sigma_{n=0}^{\infty} 2 e^{-\beta_{h/c} E'_n}, \tag{2}$$

where E'_n is the degenerate energy level and the prefactor 2 in the above equation is written due to the insertion of the barrier.

With the help of the thermodynamic relation $U = -\frac{\partial \ln Z}{\partial \beta}$, one can obtain the heat exchanges for all stages. For the isothermal process *AB*, heat exchange is given by

$$Q_{AB} = U_B - U_A + k_B T_h \ln Z_B - k_B T_h \ln Z_A, \tag{3}$$

where U_A and U_B correspond to internal energies of the boxes *A* and *B*. For the isothermal process *CD*, the heat exchange is given by

$$Q_{CD} = U_D - U_C + k_B T_c \ln Z_D - k_B T_c \ln Z_C, \tag{4}$$

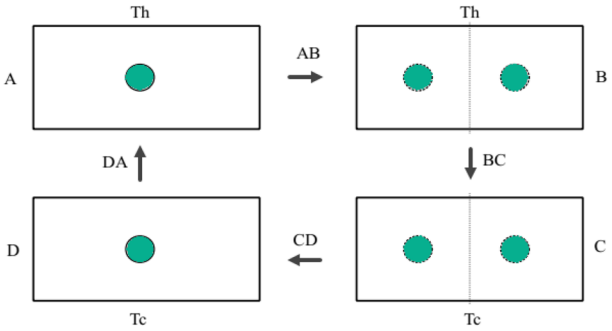


Fig. 1 Schematic picture of the Szilard-like quantum heat engine. The systems A and B at hot temperature T_h and systems C and D at the cold temperature T_c

where U_C and U_D are the internal energies of the boxes C and D. In contrast to the classical Szilard heat engine, change in internal energy does not vanish since energy levels change due to barrier insertion in a quasistatic manner. For the isochoric processes BC and DA, the corresponding heat exchanges are given by

$$Q_{BC} = U_C - U_B, \tag{5}$$

$$Q_{DA} = U_A - U_D, \tag{6}$$

respectively. The total work obtained from the cycle is given

$$W_{tot} = Q_{AB} + Q_{BC} + Q_{CD} + Q_{DA} = k_B T_h \ln \frac{Z_B}{Z_A} - k_B T_c \ln \frac{Z_C}{Z_D} \tag{7}$$

Finally, we can define the efficiency of cycle as follows:

$$\eta = \frac{W_{tot}}{Q_{supp}} = 1 + \frac{Q_{BC} + Q_{CD}}{Q_{DA} + Q_{AB}}. \tag{8}$$

Here, by using (7) and (8) we will discuss work and efficiency, respectively.

3 Positive Oscillator-shaped Well Potential

Before delving into computations we take a quick glimpse at Ref. [58]. The authors studied the solutions of position dependent mass Schrödinger equation for the harmonic oscillator-shaped well potential in Ref. [58]. They found two solutions. In order to obtain the solutions, they replaced constant particle mass m with position dependent mass $M(x)$. Moreover, the replacement of non-relativistic momentum operator and m leads to following substitutions [76]

$$-\frac{\hbar^2}{2m}\frac{d^2}{dx^2} \to -\frac{\hbar^2}{2}\frac{d}{dx}\frac{1}{M(x)}\frac{d}{dx}. \tag{9}$$

Employing the (9) into Schrödinger equation yields [58]

$$\left[-\frac{\hbar^2}{2M(x)}\frac{d^2}{dx^2} + \frac{\hbar^2}{2}\frac{M'}{M^2}\frac{d}{dx} + V(x)\right]\psi(x) = E\psi(x), \tag{10}$$

where prime denotes the derivative with respect to x. This equation can be solved analytically if one properly defines the potential $V(x)$ and $M(x)$.

3.1 Semi-infinite Quantum Well Case

First, we consider the system that is confined from the right side at a position $x = a > 0$ with an infinitely high wall. Choosing $V(x) = \frac{1}{2}M(x)\omega^2 x^2$ and $M(x) = \frac{am}{x-a}$ yields the nth energy levels as follows [58]:

$$E_n = \hbar\omega\left(n + \frac{1}{2}\right) + 2m\omega^2 a^2, \tag{11}$$

where ω is the angular frequency. From the above equation and (1), the partition functions $Z(A)$ and $Z(D)$ of the particle in boxes A and D are given by

$$Z_{A/D} = \frac{1}{2} e^{-\frac{2a^2 m\omega^2}{k_B T_{h/c}}} csch\left(\frac{\hbar\omega}{2k_B T_{h/c}}\right). \tag{12}$$

The corresponding internal energies U_A and U_D are given by

$$U_{A/D} = \frac{1}{2}\hbar\omega\left[\frac{4a^2 m\omega}{\hbar} + \coth\left(\frac{\hbar\omega}{2k_B T_{h/c}}\right)\right], \tag{13}$$

where we use the thermodynamic relations $U_{A/D} = -\frac{\ln Z_{A/D}}{\beta_{h/c}}$. On the other hand, degenerate energy levels for the boxes C and D are given by

$$E'_n = \hbar\omega\left(2n + \frac{3}{2}\right) + 2m\omega^2 a^2. \tag{14}$$

For the degenerate energy levels, the partition functions $Z(B)$ and $Z(C)$ of boxes B and C are given by

$$Z_{B/C} = e^{\frac{\omega(\hbar - 4a^2 m\omega)}{2k_B T_{h/c}}}\left[\coth\left(\frac{\hbar\omega}{k_B \mathrm{T}_{h/c}}\right) - 1\right]. \tag{15}$$

Thus, the internal energies of boxes B and C are

$$U_{B/C} = \frac{1}{2}\hbar\omega\left[\frac{4a^2 m\omega}{\hbar} + 2\coth\left(\frac{\hbar\omega}{k_B T_{h/c}}\right) + 1\right], \tag{16}$$

respectively. Finally, we get exchanged heats for all stages form (3)-(6)

$$Q_{AB} = \frac{\hbar\omega}{2}\left[\frac{2k_B T_h}{\hbar\omega}\ln\left(\frac{2}{e^{\frac{\hbar\omega}{k_B T_h}} + 1}\right) + \tanh\left(\frac{\hbar\omega}{2k_B T_h}\right) + 1\right], \tag{17}$$

$$Q_{BC} = \hbar\omega\left[\coth\left(\frac{\hbar\omega}{k_B T_c}\right) - \coth\left(\frac{\hbar\omega}{k_B T_h}\right)\right], \tag{18}$$

$$Q_{CD} = \frac{\hbar\omega}{2}\left[\frac{2k_B T_c}{\hbar\omega}\ln\left(\frac{e^{\frac{\hbar\omega}{k_B T_c}} + 1}{2}\right) - \tanh\left(\frac{\hbar\omega}{2k_B T_c}\right) - 1\right], \tag{19}$$

$$Q_{DA} = \frac{1}{2}\hbar\omega\left[\coth\left(\frac{\hbar\omega}{2k_B T_h}\right) - \coth\left(\frac{\hbar\omega}{2k_B T_c}\right)\right]. \tag{20}$$

Using (7) and (8), we get total work and efficiency

$$W_{tot} = k_B\left[T_c \ln\left(\frac{1 + e^{\frac{\hbar\omega}{k_B T_c}}}{2}\right) + T_h \ln\left(\frac{2}{e^{\frac{\hbar\omega}{k_B T_h}} + 1}\right)\right], \tag{21}$$

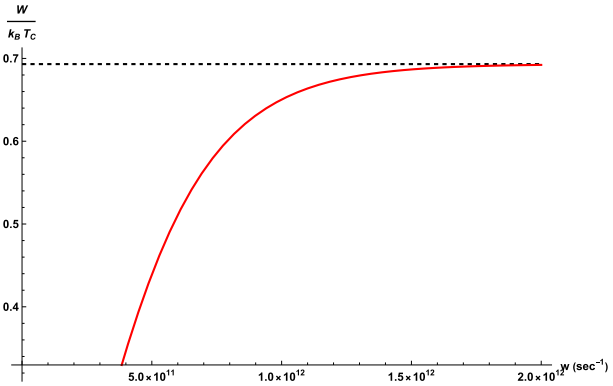


Fig. 2 Dimensionless work versus angular frequency. The dashed horizontal line corresponds to the classical limit. We take $m = 9.11 \times 10^{-31}$kg, $T_h = 2$K and $T_c = 1$K

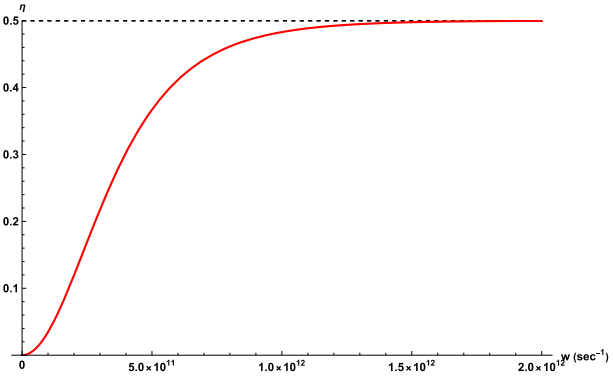


Fig. 3 Efficiency versus angular frequency. The dashed horizontal line corresponds to the classical limit. We take $m = 9.11 \times 10^{-31}$ kg, $T_h = 2$K and $T_c = 1$K

$$\eta = \frac{2k_B\left[T_c \ln\left(\frac{e^{\frac{\hbar\omega}{k_B T_c}}+1}{2}\right) + T_h \ln\left(\frac{2}{e^{\frac{\hbar\omega}{k_B T_h}}+1}\right)\right]}{\hbar\omega\left[2\coth\left(\frac{\hbar\omega}{k_B T_h}\right) + \frac{2k_B T_h}{\hbar\omega}\ln\left(\frac{2}{e^{\frac{\hbar\omega}{k_B T_h}}+1}\right) - \coth\left(\frac{\hbar\omega}{2k_B T_c}\right) + 1\right]}, \tag{22}$$

respectively.

In Figs. 2 and 3, we present the dimensionless work and efficiency with respect to angular frequency. As can be seen in (21) and (22), the dimensionless work and efficiency do not depend on the position. Both dimensionless work and efficiency reach the classical limit for the bigger values of angular frequency. Moreover, one can verify those results for (21) and (22) in the limit $\omega \to \infty$. At this point, we give some comments on large angular frequency limit. Since efficiency approaches the Carnot limit, Stirling cycle becomes reversible. Total entropy change, $dS = \frac{\delta Q_{rev}}{T}$, vanishes for large angular frequency. From (17)-(20), one finds $S_{AB} = k_B \ln 2$, $S_{BC} = 0$, $S_{CD} = -k_B \ln 2$, and $S_{DA} = 0$ in the limit $\omega \to \infty$. Thus total entropy change vanishes. We also note that both work and efficiency vanish in the limit $\omega \to 0$ since all terms in (11) depend on ω.

In Figs. 4 and 5, we show the variations of dimensionless work and efficiency with respect to temperature. Apart from Carnot case, efficiency has an upper bound [53]. Both work and efficiency approach Carnot limit for low temperature while both deviate from classical limit for high temperature.

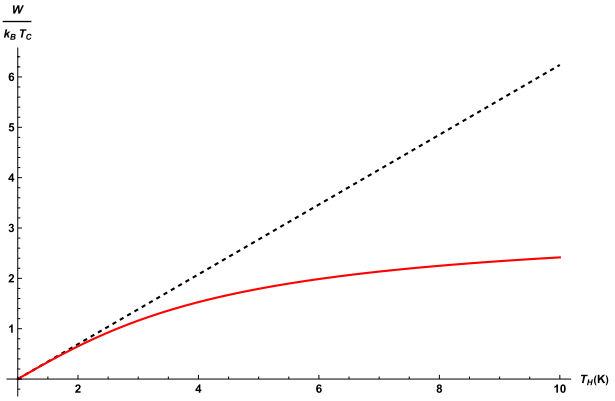


Fig. 4 Dimensionless work versus temperature. The dashed black line corresponds to the classical limit. We take $m = 9.11 \times 10^{-31}$kg, $\omega = 10^{12} sec^{-1}$ and $T_c = 1$K

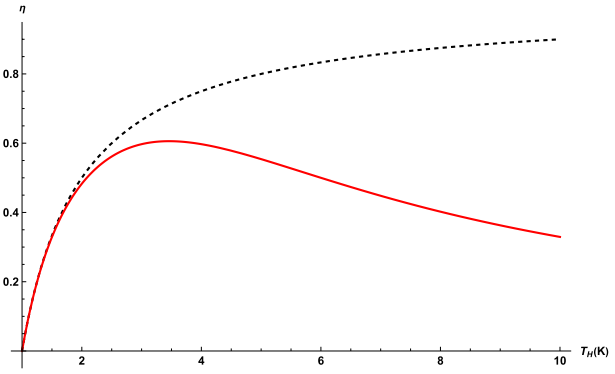


Fig. 5 Efficiency versus temperature. The dashed black line corresponds to the classical limit. We take $m = 9.11 \times 10^{-31}$kg, $\omega = 10^{12} sec^{-1}$ and $T_c = 1$K

3.2 Infinite Quantum Well Case

For a more general case where the system bounded by infinite high walls, i.e., $b > x > a$, we choose $V(x) = \frac{1}{2}M(x)\omega^2 x^2$ and $M(x) = \frac{abm}{(x-a)(b-x)}$. Then, if one solves Schrödinger equation in (10), one gets the energy levels as follows [58]:

$$E_n = \frac{b+a}{b-a}\hbar\omega\left(n+\frac{1}{2}\right) + \frac{\hbar^2}{2mab}n(n+1) + 2m\omega^2\frac{a^2b^2}{(b-a)^2}, \tag{23}$$

where $b-a$ is the width of well. The degenerate energy levels for the boxes C and D due to the insertion are given by

$$E'_n = \frac{b+a}{b-a}\hbar\omega\left(2n+\frac{3}{2}\right) + \frac{\hbar^2}{mab}(n+1)(2n+1) + 2m\omega^2\frac{a^2b^2}{(b-a)^2}. \tag{24}$$

This energy level is more complicated than (11). Since it includes a quadratic term of n, the sum of series $Z = \sum_{n=0}^{\infty} e^{-\beta E_n}$ may not be obtained analytically. So we numerically investigate partition functions.

As can be seen in Figs. 8 and 9, we present dimensionless work and efficiency with respect to angular frequency. Both reach the classical limits for the bigger values of ω. We

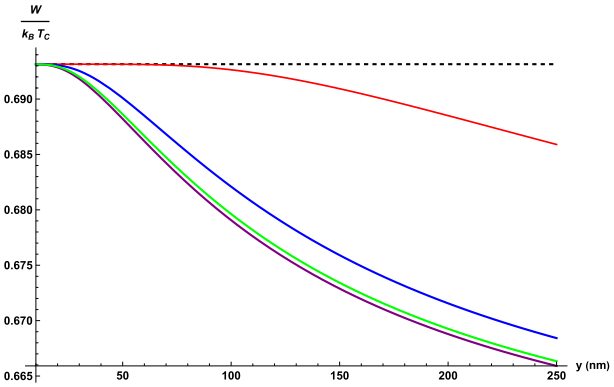


Fig. 6 Dimensionless work versus width $y = b - a$. The dashed black horizontal line corresponds to the classical limit. From top to bottom, the curves correspond to $a = 1, 4, 7, 10$nm, respectively. We take $m = 9.11 \times 10^{-31}$kg, $\omega = 10^{12}$rad sec^{-1}, $T_h = 2$K and $T_c = 1$K

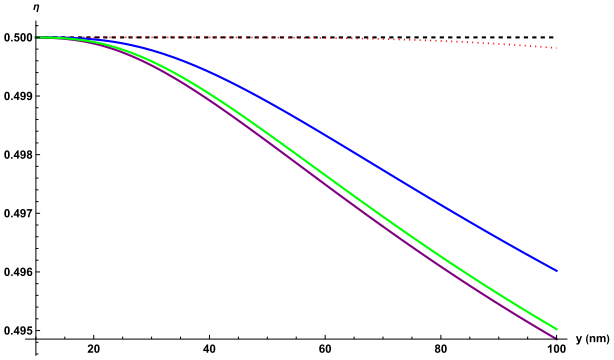


Fig. 7 Efficiency versus width $y = b - a$. The dashed black horizontal line corresponds to the classical limit. From top to bottom, the curves correspond to $a = 1, 4, 7, 10$nm, respectively. We take $m = 9.11 \times 10^{-31}$kg, $\omega = 10^{12}$rad sec^{-1}, $T_h = 2$K and $T_c = 1$K

fix $b = 30$nm and choose $a = 1, 4, 7, 10$nm. It is clearly obvious that work and efficiency decrease when we increase the value of a. Apart from semi-infinite case, both work and efficiency do not vanish for $\omega \to 0$ since the second term in (23) does not depend on ω.

We present the dimensionless work and efficiency varying with the width of well $y = b - a$ in Figs. 6 and 7, respectively. Both reach the classical limit for the smaller values of y while they deviate from the classical limit for the bigger values of y. Again, work and efficiency decrease when the values of a increase.

Finally, we show the work and efficiency with respect to temperature in Figs. 10 and 11. Similarly, they approach Carnot case for low temperature limit. Again, efficiency has a maximum value [53]. Work and efficiency decrease while a increases.

4 Discussions and Conclusions

In this paper, we have considered a Stirling-like cycle, which is based on the level degeneracy due to the barrier insertion [52], for the quantized energy levels of positive oscillator-shaped well potentials [58].

We have studied positive work and efficiency for both semi-infinite and infinite quantum well cases. For the semi-infinite case, the work and efficiency do not depend on the position a while they only depend on the angular frequency ω. For the infinite quantum well case, they depend on the position a, b, namely the width of the well $b - a$, and angular

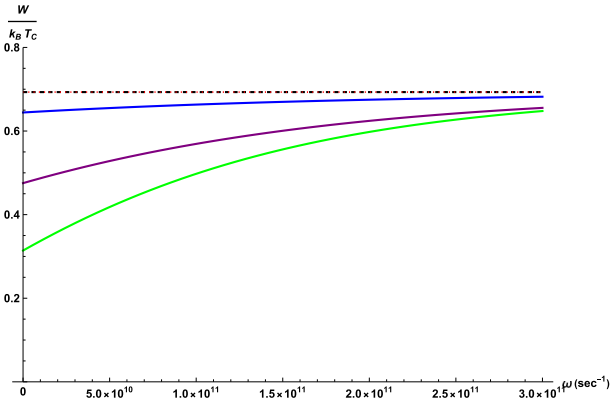


Fig. 8 Dimensionless work versus angular frequency. The dashed black horizontal line corresponds to the classical limit. From top to bottom, the curves correspond to $a = 1, 4, 7, 10$ nm, respectively. We take $m = 9.11 \times 10^{-31}$kg, $b = 30$nm, $T_h = 2$K and $T_c = 1$K

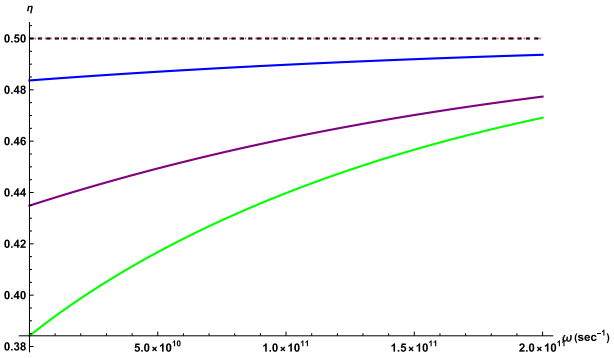


Fig. 9 Efficiency versus angular frequency. The dashed black horizontal line corresponds to the classical limit. From top to bottom, the curves correspond to $a = 1, 4, 7, 10$nm, respectively. We take $m = 9.11 \times 10^{-31}$kg, $b = 30$nm, $T_h = 2$K and $T_c = 1$K

frequency ω. In Figs. 2 and 3, we have presented total work and efficiency varying with angular frequency for the semi-infinite cases. Both approach the classical limit for the bigger values of angular frequency ω. The same behavior for the infinite case can also be seen in Figs. 8 and 9. We have shown the work and efficiency with respect to the width of the well for the infinite case in Figs. 6 and 7. Both quantities deviate from the classical limits when y increases. One can see these results are compatible with the results of Refs. [52, 53]. We have also investigated work and efficiency with respect to temperature in Figs. 4, 5, 10 and 11. Work and efficiency approach Carnot limit for low temperature while they deviate from Carnot limit for high temperature.

It should be noted that, in our calculation, we set energy degeneracy as $2n + 1$ in (14) and (24) based on Refs. [53, 54] where the eigenvalues of even energy states increase to odd energy states. Therefore, the $2n + 1$ degenerate selection has been shown to be a correct choice for the harmonic oscillator. In our case, we also set degeneracy as $2n + 1$ since the dominant term in (14) and (24) are the first terms that correspond to the energy eigenvalue of the harmonic oscillator. Other terms denote additional contributions to the energy eigenvalue.

Another point is the position-dependent mass effect on the work and efficiency for both semi-infinite and infinite quantum well. We would like to clarify this point. It can be seen that the position dependence of the mass, namely x is not included in the energy eigenvalue expressions. The boundaries come as a contribution to the energy eigenvalues. For this

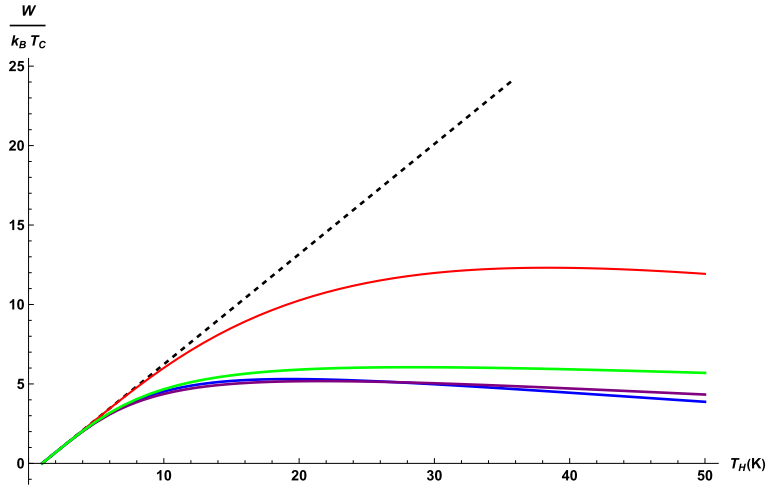


Fig. 10 Dimensionless work versus temperature. The dashed black line corresponds to the classical limit. From top to bottom, the curves correspond to $a = 1, 4, 7, 10$nm, respectively. We take $m = 9.11 \times 10^{-31}$kg, $b = 30$nm, $\omega = 10^{12} sec^{-1}$ and $T_c = 1$K

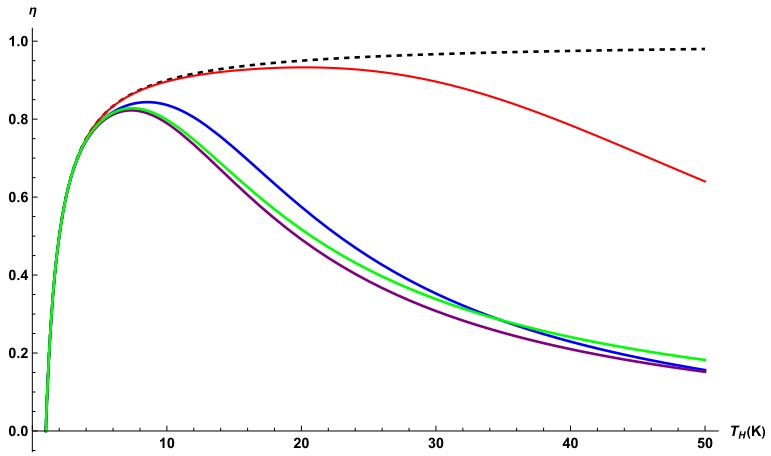


Fig. 11 Efficiency versus temperature. The dashed black line corresponds to the classical limit. From top to bottom, the curves correspond to $a = 1, 4, 7, 10$nm, respectively. We take $m = 9.11 \times 10^{-31}$kg, $b = 30$nm, $\omega = 10^{12} sec^{-1}$ and $T_c = 1$K

reason, the dependence of the mass on the position does not cause any problems in the calculations of work and efficiency in thermodynamic cycles.

Lastly, let us give some comments on the low-temperature limits of work and efficiency. One can consider energy levels in (11) and (23) as $E_n >> k_B T_h$. This condition is valid for big values of ω and small values of T_h. Thus, one may infer this condition as the low-temperature limit. The same condition can also be considered for big values of a and b, i.e. y. The work and efficiency reduce to $W \approx k_B(T_h - T_c)\ln 2$ and $\eta \approx 1 - T_c/T_h$ [52, 53] for the big values of ω, a and b.

In conclusion, we have shown that these systems produce positive work and efficiency like other models which have different potential shapes. We give some numerical results and discussions of the heat engine for the various parameters. It is well known that many physical systems are proposed as candidates as quantum heat engines, and work and efficiency are modeled in such systems. Obtained results also indicate that semiconductors [71], superlattices [72], materials of non-uniform chemical composition [73], heterostructures [74], and abrupt heterojunctions [75] can also be considered as potential candidates for a quantum heat engine.

Acknowledgements Authors thank Ramazan Sever for valuable suggestions. This work is supported by İstanbul University Post-Doctoral Research Project: MAB-2021-38032.

Author Contributions All authors contributed equally to this work.

Data Availability The datasets used and analyzed during the current study are available from the corresponding author upon reasonable request.

Declarations

Competing interests The authors declare no competing interests.

References

1. Maxwell, J.C.: Sketch of thermodynamics. In: Knott, C.G. (ed.) Life and Scientific Work of Peter Guthrie Tait, pp. 213–214. Cambridge University Press, Cambridge (1911)
2. Szilard, L.: über die entropieverminderung in einem thermodynamischen system bei eingriffen intelligenter wesen. Z. Physik **53**, 840–856 (1929). https://doi.org/10.1007/BF01341281
3. Landauer, R.: Irreversibility and heat generation in the computing process. IBM J. Res. Dev. **5**(3), 183–191 (1961). https://doi.org/10.1147/rd.53.0183
4. Bennett, C.H.: The thermodynamics of computation–a review. Int. J. Theor. Phys. **5**(3), 905–940 (1982). https://doi.org/10.1007/BF02084158
5. Leff, H., Rex, A.: Maxwell's Demon 2: Entropy, Classical and Quantum Information, Computing. Institute of Physics, London (2003)
6. Maruyama, K., Nori, F., Vedral, V.: Colloquium: the physics of maxwell's demon and information. Rev. Mod. Phys. **81**, 1–23 (2009). https://doi.org/10.1103/RevModPhys.81.1
7. Bérut, A., et al.: Experimental verification of landauer's principle linking information and thermodynamics. Nature **483**, 187 (2012). https://doi.org/10.1038/nature10872
8. Koski, J.V., et al.: Experimental realization of a szilard engine with a single electron. Proc. Natl. Acad. Sci. U.S.A. **111**, 13786–13789 (2014). https://doi.org/10.1073/pnas.1406966111
9. Serreli, V., Lee, C.-F., Kay, E.R., Leigh, D.A.: A molecular information ratchet. Nature **445**, 523–527 (2007). https://doi.org/10.1038/nature05452
10. Raizen, M.G.: Comprehensive control of atomic motion. Science **324**, 1403–1406 (2009). https://doi.org/10.1126/science.1171506
11. Bannerman, S.T., Price, G.N., Viering, K., Raizen, M.G.: Single-photon cooling at the limit of trap dynamics: Maxwell's demon near maximum efficiency. New J. Phys. **11**(6), 063044 (2009). https://doi.org/10.1088/1367-2630/11/6/063044
12. Koski, J.V., Maisi, V.F., Sagawa, T., Pekola, J.P.: Experimental observation of the role of mutual information in the nonequilibrium dynamics of a maxwell demon. Phys. Rev. Lett. **113**(5), 030601 (2014). https://doi.org/10.1103/PhysRevLett.113.030601
13. Koski, J.V., Kutvonen, A., Khaymovich, I.M., Ala-Nissila, T., Pekola, J.P.: On-chip maxwell's demon as an information-powered refrigerator. Phys. Rev. Lett. **115**(5), 260602 (2015). https://doi.org/10.1103/PhysRevLett.115.260602
14. Vinjanampathy, S., Anders, J.: Quantum thermodynamics. Contemp. Phys. **57**(4), 545–579 (2016). https://doi.org/10.1080/00107514.2016.1201896

15. Bhattacharjee, S., Dutta, A.: Quantum thermal machines and batteries. Eur. Phys. J. B **94**, 239 (2021). https://doi.org/10.1140/epjb/s10051-021-00235-3
16. Scovil, H.E.D., Schulz-DuBois, E.O.: Three-level masers as heat engines. Phys. Rev. Lett., 2 **2**, 262–263 (1959). https://doi.org/10.1103/PhysRevLett.2.262
17. Quan, H.T., Liu, Y.-X., Sun, C.P., Nori, F.: Quantum thermodynamic cycles and quantum heat engines. Phys. Rev. E **76**(18), 031105 (2007). https://doi.org/10.1103/PhysRevE.76.031105
18. Mahler, G.: Quantum Thermodynamic Processes: Energy and Information Flow at the Nanoscale. Pan Stanford Publ., Singapore (2015)
19. Quan, H.T.: Quantum thermodynamic cycles and quantum heat engines. ii. Phys. Rev. E **79**(10), 041129 (2009). https://doi.org/10.1103/PhysRevE.79.041129
20. Chen, L., Liu, X., Wu, F., Xia, S., Feng, H.: Exergy-based ecological optimization of an irreversible quantum carnot heat pump with harmonic oscillators. Phys. A **537**, 122597 (2020). https://doi.org/10.1016/j.physa.2019.122597
21. Tajima, H., Hayashi, M.: Finite-size effect on optimal efficiency of heat engines. Phys. Rev. E **96**(38), 012128 (2017). https://doi.org/10.1103/PhysRevE.96.012128
22. Wang, H., Liu, S., He, J.: Performance analysis and parametric optimum criteria of a quantum otto heat engine with heat transfer effects. Appl. Therm. Eng. **29**(4), 706–711 (2009). https://doi.org/10.1016/j.applthermaleng.2008.03.042
23. Stefanatos, D.: Optimal efficiency of a noisy quantum heat engine. Phys. Rev. E **90**(5), 012119 (2014). https://doi.org/10.1103/PhysRevE.90.012119
24. Wu, F., Chen, L., Sun, F., Wu, C., Li, Q.: Generalized model and optimum performance of an irreversible quantum brayton engine with spin systems. Phys. Rev. E **73**(7), 016103 (2006). https://doi.org/10.1103/PhysRevE.73.016103
25. Dong, C.D., Lefkidis, G., Hubner, W.: Magnetic quantum diesel engine in ni_2. Phys. Rev. B **88**(11), 214421 (2013). https://doi.org/10.1103/PhysRevB.88.214421
26. Dinis, L., et al.: Thermodynamics at the microscale: from effective heating to the brownian carnot engine. J. Stat. Mech., 054003 (2016). https://doi.org/10.1088/1742-5468/2016/05/054003
27. Agarwal, G.S., Chaturvedi, S.: Quantum dynamical framework for brownian heat engines. Phys. Rev. E **88**(12), 012130 (2013). https://doi.org/10.1103/PhysRevE.88.012130
28. Aydiner, E., Han, S.D.: Quantum heat engine model of mixed triangular spin system as a working substance. Phys. A **509**, 766–776 (2018). https://doi.org/10.1016/j.physa.2018.06.018
29. Zhang, X.Y., Huang, X.L., Yi, X.X.: Quantum otto heat engine with a non-markovian reservoir. J. Phys. A: Math. Theor. **47**(45), 455002 (2014). https://doi.org/10.1088/1751-8113/47/45/455002
30. Scully, M.O., Zubairy, M.S., Agarwal, G.S., Walther, H.: Extracting work from a single heat bath via vanishing quantum coherence. Science **299**, 862–864 (2003). https://doi.org/10.1126/science.1078955
31. Quan, H.T., Zhang, P., Sun, C.P.: Quantum-classical transition of photon-carnot engine induced by quantum decoherence. Phys. Rev. E **73**(6), 036122 (2006). https://doi.org/10.1103/PhysRevE.73.036122
32. Huang, X.L., Wang, T., Yi, X.X.: Effects of reservoir squeezing on quantum systems and work extraction. Phys. Rev. E **86**(6), 051105 (2012). https://doi.org/10.1103/PhysRevE.86.051105
33. Roßnagel, J., Abah, O., Schmidt-Kaler, F., Singer, K., Lutz, E.: Nanoscale heat engine beyond the carnot limit. Phys. Rev. Lett. **112**(5), 030602 (2014). https://doi.org/10.1103/PhysRevLett.112.030602
34. Niedenzu, W., Mukherjee, V., Ghosh, A., Kofman, A.G., G., K.: Quantum engine efficiency bound beyond the second law of thermodynamics. Nat. Commun. **9**, 165 (2018). https://doi.org/10.1038/s41467-017-01991-6
35. Wang, J., He, J., Ma, Y.: Finite-time performance of a quantum heat engine with a squeezed thermal bath. Phys. Rev. E **100**(8), 052126 (2019). https://doi.org/10.1103/PhysRevE.100.052126
36. Dillenschneider, R., Lutz, E.: Energetics of quantum correlations. EPL **88**(5), 50003 (2009). https://doi.org/10.1209/0295-5075/88/50003
37. Geva, E., Kosloff, R.: A quantum-mechanical heat engine operating in finite time. a model consisting of spin-1/2 systems as the working fluid. J. Chem. Phys. **96**, 3054 (1992). https://doi.org/10.1063/1.461951
38. Harbola, U., Rahav, S., Mukamel, S.: Quantum heat engines: a thermodynamic analysis of power and efficiency. EPL **99**, 50005 (2012). https://doi.org/10.1209/0295-5075/99/50005
39. Rahav, S., Harbola, U., Mukamel, S.: Heat fluctuations and coherences in a quantum heat engine. Phys. Rev. A **86**(8), 043843 (2012). https://doi.org/10.1103/PhysRevA.86.043843
40. Su, S., Zhang, Y., Su, G., Chen, J.: The carnot efficiency enabled by complete degeneracies. Phys. Lett. A **382**(32), 2108–2112 (2018). https://doi.org/10.1016/j.physleta.2018.05.042
41. Lin, B., Chen, J.: Performance analysis of an irreversible quantum heat engine working with harmonic oscillators. Phys. Rev. E **67**(8), 046105 (2003). https://doi.org/10.1103/PhysRevE.67.046105

42. Lin, B., Chen, J.: Optimization on the performance of a harmonic quantum brayton heat engine. J. Appl. Phys. **94**, 6185–6191 (2003). https://doi.org/10.1063/1.1616983
43. Insinga, A., Andresen, B., Salamon, P.: Thermodynamical analysis of a quantum heat engine based on harmonic oscillators. Phys. Rev. E **94**(10), 012119 (2016). https://doi.org/10.1103/PhysRevE.94.012119
44. Kosloff, R., Rezek, Y.: The quantum harmonic otto cycle. Entropy **19**, 136 (2017). https://doi.org/10.3390/e19040136
45. Kim, S.V., et al.: Quantum szilard engine. Phys. Rev. Lett. **106**(4), 070401 (2011). https://doi.org/10.1103/PhysRevLett.106.070401
46. Li, H., Zou, J., Li, J.-G., Shao, B., Wu, L.-A.: Quantum isothermal reversible process of particles in a box with a delta potential. J. Korean Phys. Soc. **66**(6), 739–743 (2015). https://doi.org/10.3938/jkps.66.739
47. Cai, C.Y., Dong, H., Sun, C.P.: Multiparticle quantum szilard engine with optimal cycles assisted by a maxwell's demon. Phys. Rev. E **85**(12), 031114 (2012). https://doi.org/10.1103/PhysRevE.85.031114
48. Zhuang, Z., Liang, S.-D.: Quantum szilard engines with arbitrary spin. Phys. Rev. E **90**(11), 052117 (2014). https://doi.org/10.1103/PhysRevE.90.052117
49. Bengtsson, J., et al.: Quantum szilard engine with attractively interacting bosons. Phys. Rev. Lett. **120**(5), 100601 (2018). https://doi.org/10.1103/PhysRevLett.120.100601
50. Park, J.J., et al.: Heat engine driven by purely quantum information. Phys. Rev. Lett. **111**(5), 230402 (2013). https://doi.org/10.1103/PhysRevLett.111.230402
51. Mehta, V., Johal, R.S.: Quantum otto engine with exchange coupling in the presence of level degeneracy. Phys. Rev. Lett. **96**(7), 032110 (2017). https://doi.org/10.1103/PhysRevE.96.032110
52. Thomas, G., Das, D., Ghosh, S.: Quantum heat engine based on level degeneracy. Phys. Rev. E **100**(7), 012123 (2019). https://doi.org/10.1103/PhysRevE.100.012123
53. Chatterjee, S., Koner, A., Chatterjee, S., Kumar, C.: Temperature-dependent maximization of work and efficiency in a degeneracy-assisted quantum stirling heat engine. Phys. Rev. E **103**(12), 062109 (2021). https://doi.org/10.1103/PhysRevE.103.062109
54. Davies, P., Thomas, L., Zahariade, G.: The harmonic quantum szilárd engine. Am. J. Phys. **89**(12), 1123–1131 (2019). https://doi.org/10.1119/10.0005946
55. Aydiner, E.: Quantum szilard engine for the fractional power-law potentials. Sci. Rep. **11**, 1576 (2021). https://doi.org/10.1038/s41598-020-80639-w
56. Aydiner, E.: Space-fractional quantum heat engine based on level degeneracy. Sci. Rep. **11**, 17901 (2021). https://doi.org/10.1038/s41598-021-97304-5
57. Zhang, H.W., Huang, X.L., Wu, S.L.: Quantum heat engine with identical particles and level degeneracy. Int. J. Mod. Phys. B, 2450109. https://doi.org/10.1142/S0217979224501091
58. Jafarov, E.I., Nagiyev, S.M.: Exact solution of the position-dependent mass schrödinger equation with the completely positive oscillator-shaped quantum well potential. https://doi.org/10.48550/arXiv.2212.13062
59. Mathews, P.M., Lakshmanan, M.: A quantum-mechanically solvable nonpolynomial lagrangian with velocity-dependent interaction. Nuovo Cim. **26**, 299–316 (1975). https://doi.org/10.1007/BF02769015
60. Schmidt, A.G.M.: Time evolution for harmonic oscillators with position-dependent mass. Phys. Scr. **75**(4), 480 (2007). https://doi.org/10.1088/0031-8949/75/4/019
61. Amir, N., Iqbal, S.: Exact solutions of schrödinger equation for the position-dependent effective mass harmonic oscillator. Commun. Theor. Phys. **62**(6), 790 (2014). https://doi.org/10.1088/0253-6102/62/6/03
62. Quesne, C.: Generalized nonlinear oscillators with quasi-harmonic behaviour: classical solutions. J. Math. Phys. **56**, 012903 (2015). https://doi.org/10.1063/1.4906113
63. Karthiga, S., et al.: Quantum solvability of a general ordered position dependent mass system: mathews-lakshmanan oscillator. J. Math. Phys. **58**, 102110 (2017). https://doi.org/10.1063/1.5008993
64. Jafarov, E.I., et al.: Exact solution of the position-dependent effective mass and angular frequency schrödinger equation: harmonic oscillator model with quantized confinement parameter. J. Phys. A: Math. Theor. **53**(48), 485301 (2020). https://doi.org/10.1088/1751-8121/abbd1a
65. Jafarov, E.I., Nagiyev, S.M., Jafarova, A.M.: Quantum-mechanical explicit solution for the confined harmonic oscillator model with the von roos kinetic energy operator. Rep. Math. Phys. **86**(1), 25–37 (2020). https://doi.org/10.1016/S0034-4877(20)30055-0
66. Jafarov, E.I., Nagiyev, S.M., Seyidova, A.M.: Dynamical symmetry of a semiconfined harmonic oscillator model with a position-dependent effective mass. https://doi.org/10.48550/arXiv.2305.11702
67. Jafarov, E.I., Nagiyev, S.M.: Exact solutions of schrödinger equation for the position-dependent effective mass harmonic oscillator. https://doi.org/10.48550/arXiv.2212.13062

68. Nagiyev, S.M.: On two direct limits relating pseudo-jacobi polynomials to hermite polynomials and the pseudo-jacobi oscillator in a homogeneous gravitational field. Theor. Math. Phys. **210**, 121–134 (2022). https://doi.org/10.1134/S0040577922010093
69. Nagiyev, S.M., et al.: Exactly solvable model of the linear harmonic oscillator with a position-dependent mass under external homogeneous gravitational field. European Phys. J. Plus **62**(5), 540 (2022). https://doi.org/10.1140/epjp/s13360-022-02715-6
70. Jafarov, E.I., Nagiyev, S.M.: On the exactly-solvable semi-infinite quantum well of the non-rectangular step-harmonic profile. Quantum Stud.: Math. Found **9**, 387–404 (2022). https://doi.org/10.1007/s40509-022-00275-z
71. Ross, O.: Position-dependent effective masses in semiconductor theory. Phys. Rev. B **27**, 7547–7552 (1983). https://doi.org/10.1103/PhysRevB.27.7547
72. Smith, D.L., Mailhiot, C.: Theory of semiconductor superlattice electronic structure. Rev. Mod. Phys. **62**, 173–234 (1990). https://doi.org/10.1103/RevModPhys.62.173
73. Barranco, M., Pi, M., Gatica, S.M., Hernández, E.S., Navarro, J.: Structure and energetics of mixed ^{4}he-^{3}he drops. Phys. Rev. B **56**, 8997–9003 (1997). https://doi.org/10.1103/PhysRevB.56.8997
74. Einevoll, G.T.: Operator ordering in effective-mass theory for heterostructures ii. strained systems. Phys. Rev. B **42**, 3497–3502 (1990). https://doi.org/10.1103/PhysRevB.42.3497
75. Morrow, R.A.: Establishment of an effective-mass hamiltonian for abrupt heterojunctions. Phys. Rev. B **35**, 8074–8079 (1987). https://doi.org/10.1103/PhysRevB.35.8074
76. BenDaniel, D.J., Duke, C.B.: Space-charge effects on electron tunneling. Phys. Rev. **152**, 683–692 (1966). https://doi.org/10.1103/PhysRev.152.683

Publisher's Note Springer Nature remains neutral with regard to jurisdictional claims in published maps and institutional affiliations.

Springer Nature or its licensor (e.g. a society or other partner) holds exclusive rights to this article under a publishing agreement with the author(s) or other rightsholder(s); author self-archiving of the accepted manuscript version of this article is solely governed by the terms of such publishing agreement and applicable law.